Adjustable surface plasmon resonance with Au, Ag, and Ag@Au core-shell nanoparticles

S. M. Hamidi* **and M. A. Oskuei**

Magneto-Plasmonic lab, Laser and Plasma Research Institute, Shahid Beheshti University, Tehran, Iran

**Corresponding author: m_hamidi@sbu.ac.ir*

Received November 11, 2013; accepted January 22, 2014; posted online February 28, 2014

We report an experimental study on the synthesis of metal nanoparticles (NPs) with adjustable optical density based on surface plasmon resonance (SPR). Metal NPs prepared by laser ablation in liquid method and the effect of laser parameters on the size, distribution, wavelength of SPR of Ag, Au, and mixture of Ag-Au, and Ag core/Au shell NPs are investigated. Our results show that the adjustable SPR band can be achieved in each class of NPs which is suitable for adjustable optical window applications.

OCIS codes: 160.0160, 160.4236, 120.0120, 120.4610.

doi: 10.3788/COL201412.031601.

Noble metal nanoparticles (NPs) and nanostructures are characterized by an intense and broad absorption band in the visible and near infrared range. This property is governed by the shape[1,2], size[3], background[4], composition[5], and distribution, which are described by localized surface plasmon resonance (LSPR) of NPs. LSPR is the resonance of charge density oscillations confined to metallic NPs, metal nano-clusters, and metallic nanostructures[6,7]. Have an insight to the wavelength of the LSPR in each structure has a main role in the design of plasmonic structures and as well ability to change this spectral region is a major key in the construction of tunable optical devices.

Tunable optical devices are attractive for many important operations in optical communication systems[8] and tunable wavelength filters[9]. To reach these tunable devices, the researchers have been used multilayer structures[10], optical fibers[11], chain of NPs[12], and long range surface plasmon polaritons[13].

For this purpose, single NP, mixture of NPs, and core-shell NPs have been used extensively. Since the unique wide range frequency of LSPR, core-shell NPs have been generated great interest[14]. Furthermore, preparation of these NPs can be done by the aid of many techniques such as chemical[15] and laser ablation methods[16]. In laser ablation in liquids (LAL), we can prepare single and core-shell NPs in aqueous medium which is depends on many factors such as ablation time, laser fluence, and environment aqueous medium. The study of core-shell NPs' size and surface plasmon of double metal NPs have been reported[16,17]. But dependence of distribution of the NPs, reliance of the wavelength of LSPR in the media, and the difference between duration times of each core or shell NPs and subsequently the sizes have not been widely explored.

In this letter, we have prepared Au and Ag NPs and Ag core/ Au shell (Ag@Au) NPs by LAL method and the adjustability of the wavelength of LSPR in these structures have been investigated.

Our samples prepared as three classes based on Au NPs, Ag NPs and also Ag@Au core-shell NPs which contain 3, 3, and 6 samples, respectively. The three sets of samples prepared by LAL method by the aid of first harmonic of the Nd: YAG laser with the wavelength 1064 nm, repetition rate of 10 Hz, pulse duration of 4−6 ns, and different energy per pulse was focused on the rotating samples[18].

Metallic NPs prepared after various time and different energy per pulses from pure target in the quartz cell with 10 mL de-ionized water. After preparation of Au and Ag NPs in different steps, the solutions of these colloids mix with each other and we reach to Ag-Au mixture in water environment.

On the other hand, we used Ag target to reach Ag NPs and then we replaced Ag target with the pure gold one in the quartz cell, and we had Ag core- Au shell NPs as Ag@Au NPs.

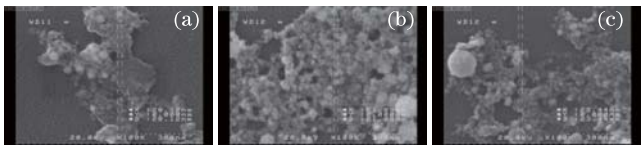

Fig. 1. SEM images of Au NPs (a) S_1, (b) S_2, and (c) S_3.

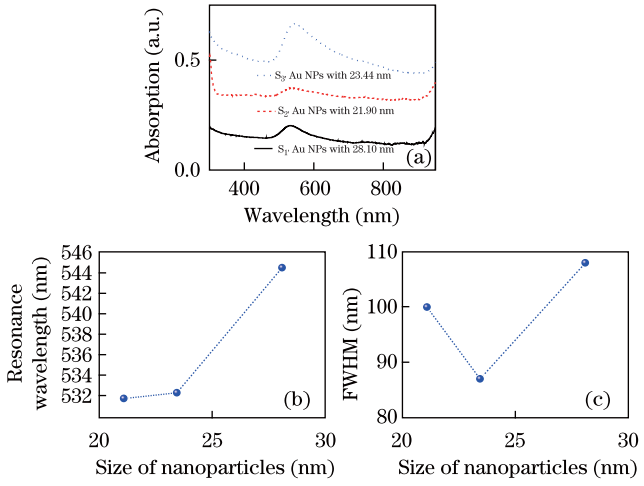

Fig. 2. (a) Absorption spectra of Au colloidal NPs with different sizes; (b) SPR wavelength and (c) FWHM of the absorption region as a function of NPs sizes.

We use scanning electron microscopy (SEM) to study the NPs' size and shapes and UV-visible spectrometer to record the optical absorption spectra.

Au NPs prepared by Nd: YAG laser under different conditions as: S_1 sample was prepared by 100 mJ energy per pulse for 1 min, and S_2 and S_3 were prepared by pulse energy of 180 mJ for 2 and 4 min, respectively. The average sizes of NPs were measured as 28.1, 21.09, and 23.44 nm for S_1, S_2, and S_3, through the mean values of five repeated SEM images from NPs on the glass substrate. Three of these SEM images are shown in Fig. 1.

Figure 2(a) shows the UV-visible absorption of the product S_1 to S_3 which indicates that each sample has a surface plasmon resonance (SPR) absorption spectrum according to their NPs sizes. The measured SPR peak of these samples indicates that the resonance peak become stronger as NPs size increases. Adjustability of the SPR wavelength of the samples takes place from 532 to 546 nm (Fig. 2(b)).

Also the full width at half maximum (FWHM) of the absorption band of the samples which indicates the distribution of NPs size is shown in Fig. 2(c).

In fact, we have been investigated the effect of different energy per pulses and also effect of different times of ablation in the preparation of Au NPs in order to use them as an absorber in the middle of visible spectral region.

Ag NPs prepared by LAL method for 2 min under different energy per pulses as S_{Ag1} with 80 mJ, S_{Ag2} with 100 mJ, and S_{Ag3} with 120 mJ. The absorption spectra of NPs with different sizes are shown in Fig. 3 (a). For these samples, Ag NPs' sizes were varied from 18.45 to 28.1 nm and the wavelength of SPR had a red shift by increasing in the NPs sizes (about 7 nm). SEM image of one of these samples onto glass substrate is shown in Fig. 4.

In spite of Au NPs, we see that in Ag NPs, we decrease in FWHM of SPR band as we increase the size of Ag NPs. Furthermore use of higher energy laser pulses yield to increase in the size of NPs. In fact, the average size of NPs prepared at 80, 100, and 120 mJ are 18.45, 25.78, and 28.10 nm, respectively, which indicates that when laser energy increases, the average size begins to increase and the concentration and subsequently absorption start to decrease.

As mentioned in the experiment, we have been prepared Ag-Au mixture by combining the NPs, which are prepared in different aqueous and then mix with each other, and the absorption spectra of these mixture of NPs have been recorded to establish the difference between them with core shell of Ag/Au (Ag@Au) NPs, which are prepared by the same irradiation time and the same energy per pulses.

It should be noted that silver NPs does not stay in high level in the water and we have fast and strong sedimentation of Ag NPs compare with Au NPs in the medium without any stabilizer. This fact resulting in Au fast aggregation and larger NPs compares with Ag NPs which is confirmed by Fig. 5(a). This fast sedimentation of Ag NPs yields to the larger NPs and hence gives rise in the absorption of it as compare with Au in the mixture state. But in the core shell state, Ag NPs give a stable state by the aid of Au NPs and we have very low aggregation

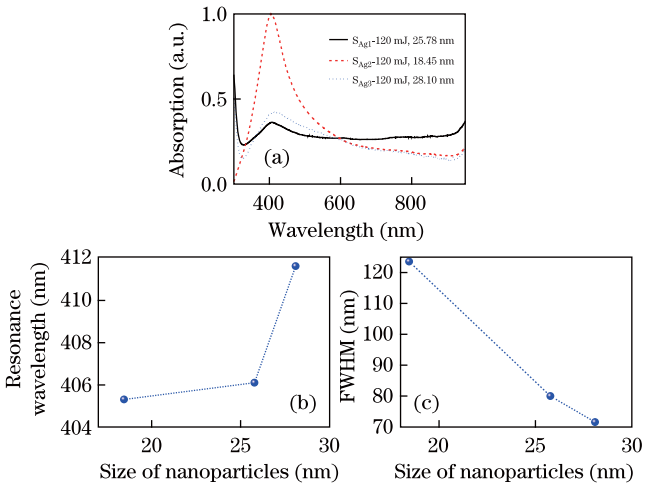

Fig. 3. (a) Absorption spectra of Ag colloidal NPs with different sizes; (b) SPR wavelength and (c) FWHM of the absorption region as a function of NPs sizes.

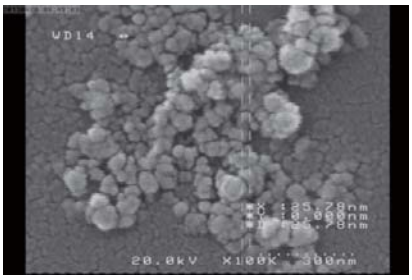

Fig. 4. SEM image of Ag NPs (S_{Ag2}).

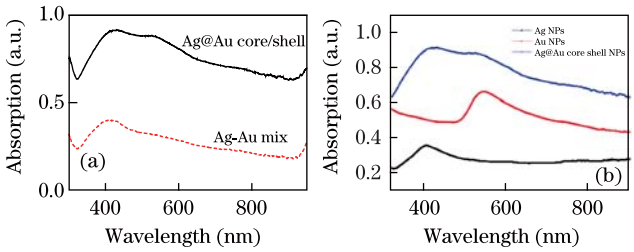

Fig. 5. Absorption spectra of (a) Ag –Au mixture and Ag@Au core shell NPs with the same irradiation time and the same laser pulses energy and (b) Ag@Au NPs as compared with each of NPs.

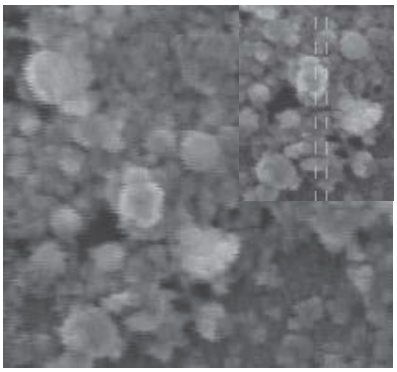

Fig. 6. SEM image of Ag@Au core shell NPs.

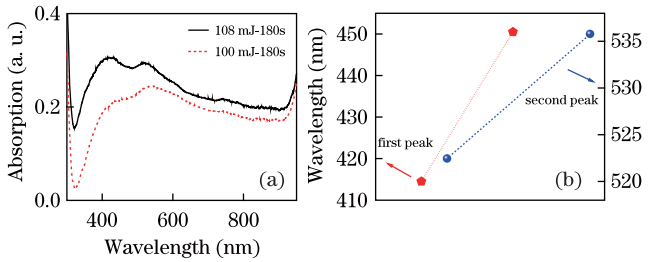

Fig. 7. (a) Absorption spectra of Ag@Au core shell NPs prepared under different energies per pulse and (b) the tuning SPR band of the first and second peaks.

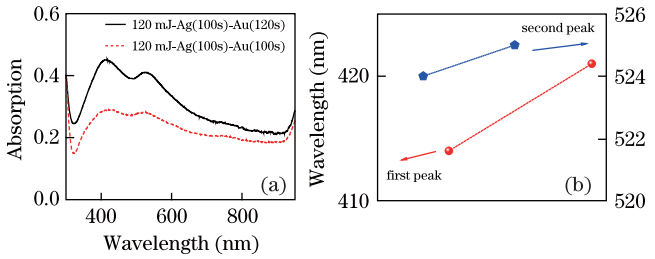

Fig. 8. (a) Absorption spectra of Ag@Au core shell NPs prepared under different times of irradiation to produce Au shell NPs and (b) the tuning SPR band of the first and second peaks.

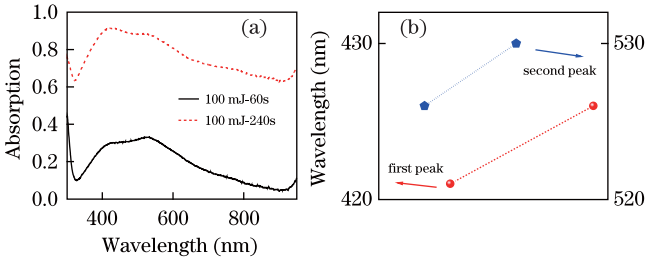

Fig. 9. (a) Absorption spectra of Ag@Au core shell NPs prepared under different irradiation times of produce each core and shell NPs and (b) the tuning SPR band of the first and second peaks.

in the water. On the other word, when we use mixture of NPs, each of them go to the stable ionic state by the aid of environmental water and in absorption spectra of them, we see one majority peaks according to the larger NPs in the aqueous medium. Also one can see the difference between absorption spectra of core shell NPs and each of pure NPs absorption spectra in Fig. 5(b). SEM image of one of the core shell NPs has been shown in Fig. 6.

In this ablating process, the laser pulse can penetrate into the surface of the gold or silver target. Because the same crystal structure of these metals and the low lattice mismatch between them, the silver atoms are able to attach the surface of gold NPs and form Ag@Au NPs as a core shell NPs. Thus we must have two peaks in absorption spectra correspond to each of metal NPs.

In fact, the SPR mode of Ag NPs interacts with Au core and can form the bonding or anti-bonding mode accordance to the thickness of shell[19,20]. In our experimental results, because the appearance of parallel dipole moment between Ag sphere and Au shell, its plasmon energy is high and it's appear in the data as a second peak.

Now, effects of different time and different irradiation energy have been investigated in Ag@Au core shell NPs in LAL method. For this purpose, in the first twin samples, we use the same time and the equal energy in ablation of Ag and Au in one core shell preparation and then the irradiation energy has been changed to study the effect of energy on the core shell sizes and then on the optical property of them (Fig. 7).

The first peak corresponds to the SPR of Ag core has been changed from 420 to 450 nm and the second one has been tuned from 524 to 536 nm. One can see that as NPs ablation energy increases, the SPR band gradually blue shifts with gradually increasing the intensity of SPR in both long and short wavelength regions.

Another set of samples were prepared under the same energy (120 mJ) and the Ag ablation time as a core in these structures has been changed from 100 to 120 s with the same ablation time (120 s) for Au shell (Fig. 8).

These figures illustrate that enhancement in the shell ablation time, influence on the first peak of SPR of the sample from 421 to 414 nm and the second peak of SPR has been changed about 1nm. Also the intensity of SPR band has been enhanced when the ablation time of the Au shell increases.

Finally effect of change in the ablation time of each core and shell NPs has been investigated in another set of samples. In the ablating process, the laser pulse with the same amount of energy, 100 mJ, has been used to ablate the Ag and Au NPs after 60 and 240 seconds. It is evident that the tunability of SPR peaks of two samples have the same amount for the first and second ones (5 nm) and we have sufficient enhancement in the intensity of SPR bands when the ablation time increases (Fig. 9).

The Ag@Au core shell structure in which the ablation time is set to 240 s is a very good candidate for use as absorbing window in the visible region.

In conclusion, the Ag, Au, Ag-Au mixture, and Ag core/ Au shell colloid NPs are prepared by LAL method. The optical density spectrum of the NPs shows the peak in absorption spectra corresponds to the SPR band which is adjusted by the aid of change in the laser parameters and then in NPs size and distributions. In Ag@Au core shell NPs, two distinct peaks correspond to SPR of each of NPs. Our results show significant adjustability and absorption band for each set of NPs that is may be useful in the design of optical absorption window.

References

1. D. E. Mostafa, T. Yang, Z. Xuan, S. Chen, H. Tu, and A. Zhang, Plasmonics **5,** 221 (2010).
2. J. Li, Q. Kan, C. Wang, and H. Chen, Chin. Opt. Lett. **9,** 090501 (2011).
3. S. M. Hamidi and M. M. Tehranchi, J. Phys. D Appl. Phys. **44,** 305003 (2011).
4. K. C. Vernon, A. M. Funston, C. Novo, D. E. Gomez, P. Mulvaney, and T. J. Davis, Nano. Lett. **10,** 2080 (2010).
5. E. Ringe, J. Zhang, M. R. Langille, K. Sohn, C. Cobley, L. Au, Y. Xia, C. A. Mirkin, J. Huang, L. D. Marks, and R. P. Van Duyne, Mat. Res. Soc. Symp. Proc. **1208,** O10-02 (2010).
6. E. Hutter and H. Fendler, Adv. Mater. **16,** 1685 (2004).

7. J. Fang, X. Zhang, S. Qin, and S. Chang, Chin. Opt. Lett. **9,** 032401 (2011).
8. Q. Xu, J. Shakya, and M. Lipson, Opt. Express **14,** 6463 (2006).
9. Q. Bing, W. Hua, and Ch. Wei, Optoelectron. Lett. **9,** 101 (2013).
10. S. M. Hamidi, A. Bananej, and M. M. Tehranchi, J. Opt. Laser Technol. **44,** 1556 (2012).
11. H. Kumazaki, Y. Yamada, H. Nakamura, S. Inaba, and K. Hane, IEEE. Photon. Technol. Lett. **13,** 1206 (2001).
12. V. V. Gozhenko, D. A. Smith, J. L. Vedral, V. V. Kravets, and A. O. Pinchuk, J. Phys. Chem. C. **115,** 8911 (2011).
13. J. Lee, F. Lu, and M. A. Belkin, in *Proceedings of CLEO 2012* QM2K.4 (2012).
14. H. Han, Y. Fang, Z. Li, and H. Xu, Appl. Phys. Lett. **92,** 023116 (2008).
15. J. Choma, A. Dziura, D. Jamiola, P. Nyga, and M. Jaroniec, Colloid Surface Physicochem. Eng. Aspect **373,** 167 (2011).
16. Y. Chen, H. Wu, Z. Li, P. Wang, L. Yang, and Y. Fang, Plasmonics **7,** 509 (2012).
17. H. Xu, Phys. Rev. B **72,** 073405 (2005).
18. S. M. Hamidi amd M. A. Oskuie, J. Supercond. Novel Mag. DOI 10.1007/s10948-013-2449-0 (2013).
19. E. Prodan, C. Radloff, N. J. Halas, and P. Nordlander, Science **302,** 419 (2003).
20. H. Xu, Phys. Rev. B **72,** 073405 (2005).